Acta Cryst. (1977). A33, 456–465

Crystal Structure and Electron Density Distribution of Deuterated 2,5-Dimethyl-3-hexyn-2,5-diol, $C_8H_2D_{12}O_2$, at 90 K

BY R. B. HELMHOLDT* AND AAFJE VOS

Laboratorium voor Structuurchemie, Rijksuniversiteit Groningen, Zernikelaan, Paddelpoel, Groningen, The Netherlands

(*Received* 30 *November* 1976; *accepted* 31 *December* 1976)

A study has been made of the crystal structure and electron density distribution of $(CD_3)_2(OH)C{-}C{\equiv}C{-}C(OH)(CD_3)_2$ by X-ray diffraction at 90 K. The intensities were measured with monochromatized Mo radiation (graphite monochromator) on a CAD4 diffractometer with the $\theta/2\theta$ step-scan technique, $(\sin\theta)/\lambda \leq 1{\cdot}0$ Å^{-1}. Care was taken to obtain a homogeneous X-ray beam and to avoid multiple diffraction. Profile analysis was used to determine the integrated peak intensities. The compound is triclinic, $P\bar{1}$, $a = 8{\cdot}483\,(3)$, $b = 9{\cdot}933\,(3)$, $c = 8{\cdot}801\,(3)$ Å, $\alpha = 95{\cdot}63\,(3)$, $\beta = 85{\cdot}57\,(3)$, $\gamma = 119{\cdot}63\,(3)°$ at 90 K, $Z = 3$. A least-squares refinement with all reflexions gave $R = 0{\cdot}045$. For the study of the deformation density the atomic parameters were determined by a least-squares refinement based on reflexions with $(\sin\theta)/\lambda > 0{\cdot}70$ Å^{-1}. The $[F_o - F_c(\mathrm{HO})]$ map was calculated with the reflexions having $(\sin\theta)/\lambda < 0{\cdot}65$ Å^{-1}. Deformation density maxima of 0·58 and 0·36 e Å^{-3}, $\sigma = 0{\cdot}025$ e Å^{-3}, were observed for the triple and single C–C bonds respectively. At C–O the maximum is much lower, 0·09 e Å^{-3}. The integrated electron contents of the maxima are 0·28 for C≡C and 0·07 for C–C, in good agreement with the dynamical difference density calculated for a model compound by *ab initio* methods (6,3/3 GTO basis set). The lone-pair regions of the O atoms are positive with a tendency for the electrons to contract around the hydrogen bonds.

Introduction

The work described in the present paper is part of the research being done in Groningen on accurate electron density distributions in single, double and triple C–C bonds. The series of compounds studied is

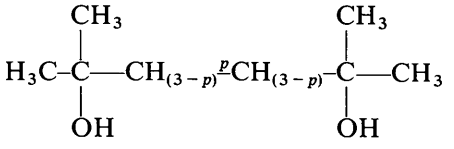

where $p = 1$, 2 or 3 for a single, double or triple bond. From earlier structure determinations (Helmholdt, Ruysink, Reynears & Kemper, 1972; Ruysink & Vos, 1974*a*; Helmholdt & Reynaers, 1976) we concluded that the crystals are of sufficient quality for accurate work. The present paper describes the structure determination and interpretation of the electron density distribution for the compound with $p = 3$. The deuterated compound in which the CH_3 groups are replaced by CD_3 groups was used. This compound will be referred to as III-D.

Synthesis and crystallization

For the X-ray diffraction work the deuterated compound was chosen as inelastic neutron diffraction work might have been necessary to determine the dispersion curves of the crystal. These curves can be used for the calculation of the errors in the intensities due to thermal diffuse scattering. Except for some minor modifications the D compound was synthesized according to the method described by Mildner & Weedon (1953) for the H analogue:

$$2C_2H_5Br + Mg \rightarrow 2C_2H_5MgBr$$

$$2C_2H_5MgBr + HC{\equiv}CH \rightarrow BrMgC{\equiv}CMgBr + 2C_2H_6$$

$$BrMgC{\equiv}CMgBr + 2CD_3COCD_3 \rightarrow (CD_3)_2C(OMgBr)C{\equiv}CC(OMgBr)(CD_3)_2$$

$$\xrightarrow{DCl/D_2O} (CD_3)_2C(OD)C{\equiv}CC(OD)(CD_3)_2 + 2MgClBr. \qquad (B)$$

As the easy exchange of hydroxyl D by H atoms will vary the D content with time, the OD groups in *B* were converted to OH groups by dissolving *B* repeatedly in acetone and evaporating the solvent. The %D in CD_3 was found to be $97 \pm 0{\cdot}5\%$ by PMR methods.

Good crystals were obtained by slowly cooling a hot saturated solution of III-D in ether: *n*-petane, 2:1.

* Present address: Netherlands Energy Research Foundation (ECN), Petten (N.H.), The Netherlands.

Experimental

A crystal of good quality with a small mosaic spread (<0·2°; Helmholdt & Vos, 1976) and a maximum dimension of 0·48 mm was chosen. To obtain accurate intensities a monochromatic homogeneous X-ray beam (Mo radiation) was used, multiple diffraction was avoided as much as possible and profile analysis was done to determine the correct peak width.

Monochromatization of X-ray beam

A pyrolytic graphite monochromator M (reflecting plane 002, $\theta=6{\cdot}1°$, mosaic spread 0·5°) was placed between the X-ray source and the crystal. This device caused the incident beam to be inhomogeneous, however, in the direction $\mathbf{r}_2$ (Fig. 1). At the position of the crystal the intensity distribution of the beam along $\mathbf{r}_2$ was dumb-bell shaped (half width 0·8 mm). The central part of the dumb-bell could be flattened by absorption of the X-rays by a (cylindrical) glass rod placed parallel to $\mathbf{r}_1$ in the beam. In this way a plateau which was homogeneous within 1% over a distance of 0·5 mm along $\mathbf{r}_2$ was obtained (de Boer, 1974). The value 0·03 obtained for $\Delta\lambda/\lambda$ is much better than for balanced filters ($\Delta\lambda/\lambda=0{\cdot}05$; Verschoor, 1967). For the polarization factor the formula given by Azaroff (1955; $\varrho=90°$ in our case) was applied:

$$P(\theta)=(1-k)\frac{\cos^2 2\theta_c+\cos^2 2\theta_M}{1+\cos^2 2\theta_M}+k\frac{\cos^2 2\theta_C+|\cos 2\theta_M|}{1+|\cos 2\theta_M|},$$

θ_M and θ_C being the glancing angles for the monochromator and the crystal respectively. For our device $P(\theta)$ does not depend much on k. The value 0·65 measured for k by Hope (1971) was tentatively assumed to be correct for our monochromator. The error due to a wrong choice of k is maximal 0·8% (in the case $k=$ 0·00).

Treatment of multiple diffraction

The occurrence of multiple diffraction has been described by Coppens (1968): his formula (1) shows that the effect is small for high-order reflexions $\mathbf{H}_1$. In this case either $\mathbf{H}_2$ or $\mathbf{H}_3$, with $\mathbf{H}_3=\mathbf{H}_1-\mathbf{H}_2$, is also of high order, giving small values for the reflecting powers r_{01} and either r_{02} or r_{23}. To avoid errors due to multiple diffraction the intensities of the reflexions hkl were measured for three different azimuth angles (−5, 0 and 5°). For $(\sin\theta)/\lambda>0{\cdot}565$ Å^{-1} the average of the three intensities was taken. For $(\sin\theta)/\lambda\leq 0{\cdot}565$ Å^{-1} the program *MULREF* was used to check whether the intensities were affected by multiple diffraction. As reflexions $\mathbf{H}_2$ (Coppens, 1968) the 84 strongest reflexions were considered. For 94% of the measured intensities *MULREF* indicated the presence of multiple diffraction. This high percentage is due to the Ewald sphere having a large radius $1/\lambda$. In many cases more than one reflexion $\mathbf{H}_2$ lies on the Ewald sphere simultaneously with $\mathbf{H}_1$. As the resulting changes in the intensity of $\mathbf{H}_1$ may (partly) cancel each other, the following procedure was used to eliminate large net errors due to multiple diffraction.

Each individual intensity was compared with the average value of the set of three measured intensities. For 6·2% of the sets differences larger than 2·5 times the standard deviation in the difference occurred. With the aid of *MULREF* for 46 intensities the difference could be ascribed to multiple diffraction. After the 46 intensities had been removed from the list, for each reflexion hkl the intensity was obtained by taking the average value of the remaining intensities of the corresponding set.

The laborious procedure described above suggests that the occurrence of multiple diffraction should be avoided by on-line procedures during the intensity measurement.

Profile analysis

To determine the background as close to the peak as possible the step-scan technique was used, each scan range being divided into 96 equal steps. Before analysis of the profiles the measured data were smoothed (Whittaker & Robinson, 1949; $\varepsilon=0{\cdot}01$). For the strongest reflexions (15%) the smoothing was used only for the flanks of the peaks as the procedure did not work well for the central part of the peaks. Peak intensities were calculated as the sum of the unsmoothed step intensities.

If after smoothing none of the step intensities was larger than $P_{\min}+2\sigma(P_{\min})$, $P_{\min}$ being the minimum step intensity, or if the maximum of the profile was not within 10 steps from the calculated reflexion position, the net integrated intensity was set equal to zero. Apart from accounting for the $K\alpha$ doublet, the first minimum seen either on the left or the right of the central part of the smoothed profile was considered as the end point of the peak. The background on the left (right) was calculated as the average of the unsmoothed intensities of the steps beyond the end point of the peak.

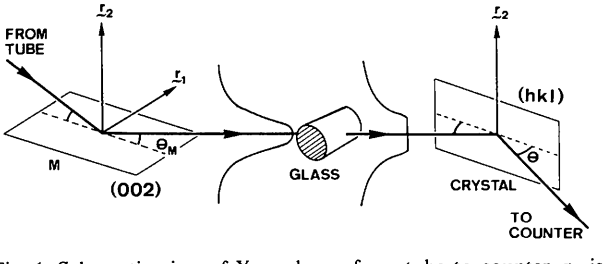

Fig. 1. Schematic view of X-ray beam from tube to counter. $\mathbf{r}_1$ is parallel to the reflecting plane of M and perpendicular to the beam reflected by M, $\mathbf{r}_2$ is parallel to the diffracting plane and perpendicular to $\mathbf{r}_1$. For further explanation see the text.

Table 1. *Experimental details*

Temperature	90 K		Crystal dimensions max.	0·48 mm
$(\sin\theta_{max})/\lambda$	1·0 Å^{-1}		Number of boundary planes	13
Radiation	Mo $K\alpha$		Mosaic spread	<0·2°
Scan method	$\theta/2\theta$		Slit width	1·265°
Scan range (°)				
$\theta<35°$	$1+2\,\mathrm{tg}\,\theta$			
$\theta>35°$	2			
Number of independent reflexions		(*a*)	10843	
of which $I_o>0$		(*b*)	8997	
of which $\lvert F_o\rvert>3\sigma_c$		(*c*)	8255	
Number of LO reflexions, $(\sin\theta)/\lambda<0{\cdot}65$ Å^{-1}		(*a*)	2950	
		(*c*)	2688	
Number of HO reflexions, $(\sin\theta)/\lambda>0{\cdot}7$ Å^{-1}		(*a*)	7156	
		(*b*)	4927	

Data collection

The profiles were collected on an Enraf–Nonius four-circle diffractometer CAD4. The crystal was cooled to 90 K by a stream of cold nitrogen gas (van Bolhuis, 1971). Experimental details are given in Table 1 and the crystallographic data in Table 2.

Table 2. *Crystallographic data at* 90 K

Space group $P\bar{1}$			
a	8·483 (3) Å†	α	95·63 (3)°
b	9·933 (3)	β	85·57 (3)
c	8·801 (3)	γ	119·63 (3)
V	641·1 Å^3	Z	3
μ(Mo)	0·837 cm^{-1}		

† Cell dimensions from diffractometer measurements.

Every hour the orientation of the crystal and the intensity of three reference reflexions were checked. The profiles were corrected for changes in intensity before analysis. The intensities were corrected for Lorentz and polarization effects and for absorption (Busing & Levy, 1957).

Structure refinement

The structure was obtained from the data collected for the H compound (Helmholdt, Ruysink, Reynaers & Kemper, 1972) by symbolic addition (Karle & Karle, 1966). There are two molecules (*A*) in general positions and one molecule (*B*) at an inversion centre. For the numbering of the atoms see Fig. 2. The structure was refined by the least-squares program of the X-RAY 1972 system (Stewart, Kruger, Ammon, Dickinson & Hall, 1972). Scale and overall temperature factors were put in one block and the parameters of *A* and *B* in second and third blocks respectively. Scattering factors for the heavy atoms were taken from Doyle & Turner (1968) and for H from Stewart, Davidson & Simpson (1968). For the heavy atoms anisotropic and for the D and H atoms isotropic temperature factors were used. Large thermal ellipsoids were found for O(1), C(2) and C(3) (Fig. 3), indicating either a large libration or static disorder about C(4)–C(5). To take the smearing of O(1), C(2) and C(3) into account each was split up into two atoms along the direction of the largest main axis of its ellipsoid. The splitting was chosen such that the remaining U value was equal to the average of the U_{ii} values of C(8), C(9) and O(10). Each D or H atom was split in the same way as the atom to which it is bound. This procedure gives, after refinement, a flat difference map in the region of the C(4) [$OH(CD_3)_2$]

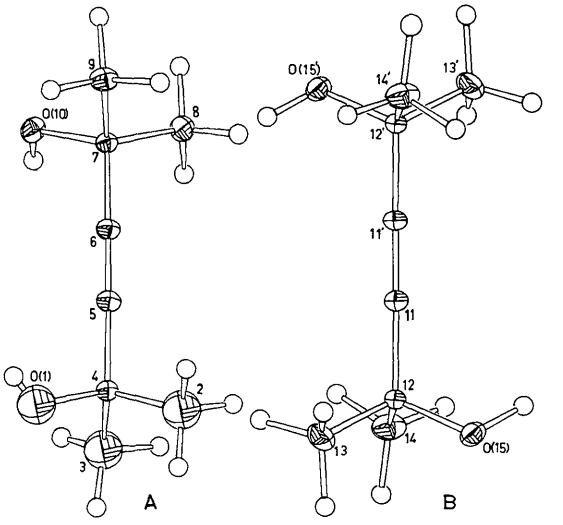

Fig. 2. Molecules of 2,5-dimethyl-3-hexyn-2,5-diol. *A* at a general position, *B* at an inversion centre.

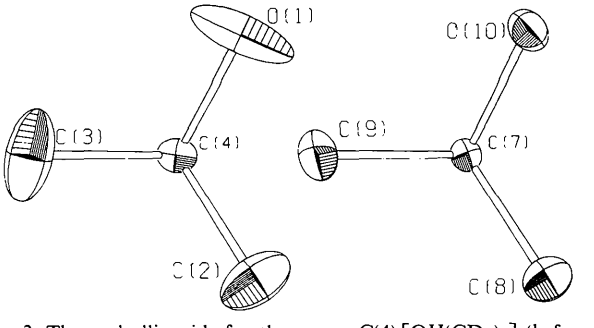

Fig. 3. Thermal ellipsoids for the group C(4) [$OH(CD_3)_2$] (before splitting) and the group C(7) [$OH(CD_3)_2$] seen along C(4)–C(5) and C(7)–C(6) respectively.

group. This region cannot be used for electron density studies, however.

During the final refinement cycles the 8255 reflexions with $|F_o| > 3\sigma(F_o)$ were considered and the positions of the H and D atoms were constrained with O–H = 0·97 and C–D = 1·08 Å. The weighting scheme was

$$w = [\sigma_c^2 + 4{\cdot}54 \times 10^{-4}|F_o|^2 - 1{\cdot}7 \times 10^{-8}|F_o|^4]^{-1},$$

where σ_c^2 is the variance in $|F_o|$ due to counting statistics. Each of the fractional atoms was given a multiplicity of 0·5. An extinction correction (Zachariasen, 1967, 1968) was not significant and was therefore not applied in the final cycles. The residuals are $R = \Sigma|F_o - F_c|/\Sigma|F_o| = 0{\cdot}045$ and $R_w = [\Sigma w(F_o - F_c)^2/\Sigma wF_o^2]^{1/2} = 0{\cdot}062$. The atomic parameters are given in Tables 3 and 4.*

High-order refinement

To keep the errors due to the assumption that the electron distribution of the static atoms is spherical as small as possible, a high-order (HO) refinement was done (O'Connell, 1969; Hanson, Sieker & Jensen, 1973) with reflexions having $(\sin\theta)/\lambda > 0{\cdot}7$ Å^{-1}. Before the refinement was started the parameters of the fractional atoms of the group C(4) [$OH(CD_3)_2$] were adjusted to the low-order (LO) reflexions, $(\sin\theta)/\lambda \leq 0{\cdot}65$ Å^{-1}, by a full-matrix least-squares refinement in which the full-angle (FA) parameters of the remaining atoms were kept constant. In the following HO refinement the LO parameters of the fractional atoms were kept fixed. In this way the deformation density map to be calculated with the LO reflexions remains flat in the neighbourhood of the disordered group. The indices

* A list of structure factors has been deposited with the British Library Lending Division as Supplementary Publication No. SUP 32409 (30 pp.). Copies may be obtained through the Executive Secretary, International Union of Crystallography, 13 White Friars, Chester CH1 1NZ, England.

Table 4. *Final atomic coordinates* ($\times 10^5$) *and thermal parameters for hydrogen and deuterium after the full-angle refinement*

	x	y	z	B (Å^2)
H(O1*a*)	58250	19025	81196	6·8 (11)
H(O1*b*)	52444	15303	77776	2·1 (4)
D(C2*a*-1)	24249	33715	82334	3·3 (7)
D(C2*a*-2)	36150	35550	95995	3·3 (6)
D(C2*a*-3)	21468	18511	88591	4·6 (8)
D(C2*b*-1)	24171	30547	81540	4·5 (8)
D(C2*b*-2)	36072	32382	95201	2·5 (6)
D(C2*b*-3)	21390	15343	87797	3·8 (7)
D(C3*a*-1)	69527	45829	64970	4·2 (9)
D(C3*a*-2)	54917	51607	66357	9·5 (16)
D(C3*a*-3)	67042	51736	81285	6·8 (12)
D(C3*b*-1)	66233	44005	64418	12·6 (22)
D(C3*b*-2)	51623	49783	65805	3·1 (7)
D(C3*b*-3)	63748	49912	80733	2·6 (7)
D(C8-1)	4593	7684	32558	2·5 (2)
D(C8-2)	11999	2274	15121	3·0 (2)
D(C8-3)	25559	20718	24116	3·0 (3)
D(C9-1)	839	−16554	43431	2·7 (2)
D(C9-2)	8794	−21829	26320	3·1 (3)
D(C9-3)	19669	−19753	43081	2·3 (2)
H(O10)	48610	12560	21205	5·6 (4)
D(C13-1)	1505	56874	64859	4·5 (3)
D(C13-2)	15006	48467	67257	4·6 (3)
D(C13-3)	24679	67577	61028	4·1 (3)
D(C14-1)	1556	77110	86776	3·6 (3)
D(C14-2)	19528	86221	98432	4·2 (3)
D(C14-3)	23486	88849	78845	3·0 (2)
H(O15)	39108	72469	98353	6·9 (4)

Table 3. *Final atomic coordinates* ($\times 10^5$) *and thermal parameters* ($\times 10^4$) *for carbon and oxygen after the full-angle refinement*

For numbering of atoms see Fig. 2. The standard deviations calculated by the least-squares program are given in parentheses. The temperature factor is defined as

$$\exp[-2\pi^2(h^2a^{*2}U_{11} + k^2b^{*2}U_{22} + l^2c^{*2}U_{33} + 2hka^*b^*U_{12} + 2klb^*c^*U_{23} + 2hla^*c^*U_{31})]$$

	x	y	z	U_{11}	U_{22}	U_{33}	U_{12}	U_{31}	U_{23}
O(1*a*)	57730 (15)	24082 (15)	81077 (13)	195 (4)	254 (5)	181 (4)	154 (4)	−44 (3)	−2 (3)
O(1*b*)	51895 (21)	20430 (17)	84548 (15)	491 (8)	345 (7)	239 (6)	330 (7)	−199 (5)	−120 (4)
C(2*a*)	30812 (65)	29438 (44)	85542 (50)	221 (7)	351 (15)	204 (9)	187 (11)	−41 (6)	−96 (10)
C(2*b*)	30987 (58)	26471 (40)	86408 (45)	175 (6)	249 (10)	144 (5)	126 (7)	1 (4)	−20 (6)
C(3*a*)	57791 (38)	45608 (31)	71241 (35)	240 (8)	144 (5)	209 (5)	75 (5)	−23 (5)	−12 (4)
C(3*b*)	61054 (39)	43780 (31)	71772 (35)	319 (12)	208 (9)	215 (7)	−53 (7)	−6 (8)	−40 (6)
C(4)	45794 (7)	28240 (6)	75125 (5)	151 (2)	150 (2)	134 (2)	82 (1)	−39 (1)	−36 (1)
C(5)	38223 (7)	18680 (6)	60908 (5)	157 (2)	157 (2)	136 (2)	77 (1)	−34 (1)	−26 (1)
C(6)	32480 (7)	11039 (5)	49108 (5)	148 (2)	138 (2)	123 (1)	66 (1)	−22 (1)	−12 (1)
C(7)	25756 (6)	1937 (5)	34452 (5)	118 (1)	110 (1)	105 (1)	49 (1)	−1 (1)	−2 (1)
C(8)	16390 (8)	8659 (6)	26038 (6)	210 (2)	197 (2)	156 (2)	127 (2)	−44 (1)	−8 (1)
C(9)	12944 (7)	−15117 (6)	37116 (6)	170 (2)	122 (2)	157 (2)	30 (1)	25 (1)	15 (1)
O(10)	40698 (5)	2508 (4)	25201 (4)	139 (1)	146 (1)	173 (1)	59 (1)	48 (1)	13 (1)
C(11)	5360 (6)	54498 (6)	95601 (5)	118 (2)	162 (2)	137 (2)	39 (1)	47 (1)	52 (1)
C(12)	17927 (6)	66027 (5)	84904 (5)	106 (1)	140 (1)	119 (1)	35 (1)	−2 (1)	43 (1)
C(13)	14568 (9)	59204 (8)	68430 (6)	283 (3)	240 (2)	117 (2)	31 (2)	−43 (2)	27 (2)
C(14)	15735 (8)	80478 (7)	87181 (7)	192 (2)	214 (2)	296 (2)	127 (2)	60 (2)	108 (2)
O(15)	36229 (5)	70026 (4)	87632 (5)	106 (1)	158 (1)	212 (2)	51 (1)	000 (1)	45 (1)

Table 5. *Final atomic coordinates* ($\times 10^5$) *and thermal parameters* ($\times 10^4$) *for carbon and oxygen after high-order refinement*

The parameters of the fractional atoms were obtained from a low-order refinement (see text).

	x	y	z	U_{11}	U_{22}	U_{33}	U_{12}	U_{31}	U_{23}
O(1*a*)	57790	24083	81016	191	264	189	152	−51	−7
O(1*b*)	51969	20467	84474	477	339	240	319	−190	−107
C(2*a*)	30351	29157	85502	248	442	185	252	−42	−96
C(2*b*)	31362	26720	86444	146	296	154	146	−31	−33
C(3*a*)	57734	45605	71150	242	159	229	65	−32	−28
C(3*b*)	61000	43860	71789	316	220	198	−48	−23	−39
C(4)	45796 (7)	28236 (6)	75120 (6)	153 (1)	152 (1)	139 (1)	84 (1)	−37 (1)	−37 (1)
C(5)	38225 (7)	18690 (6)	60930 (6)	164 (1)	161 (1)	134 (1)	79 (1)	−40 (1)	−34 (1)
C(6)	32472 (7)	11041 (6)	49096 (5)	155 (1)	144 (1)	124 (1)	69 (1)	−27 (1)	−19 (1)
C(7)	25763 (6)	1939 (5)	34446 (5)	122 (1)	113 (1)	109 (1)	51 (1)	−2 (1)	1 (1)
C(8)	16374 (9)	8646 (7)	26044 (6)	213 (2)	203 (2)	161 (1)	130 (2)	−44 (1)	−7 (1)
C(9)	12922 (8)	−15113 (6)	37110 (6)	173 (2)	128 (1)	160 (1)	34 (1)	22 (1)	15 (1)
O(10)	40699 (6)	2511 (5)	25215 (5)	142 (1)	147 (1)	176 (1)	60 (1)	46 (1)	14 (1)
C(11)	5378 (7)	54507 (6)	95577 (6)	121 (1)	165 (1)	143 (1)	38 (1)	10 (1)	61 (1)
C(12)	17943 (6)	66025 (6)	84906 (5)	112 (1)	142 (1)	121 (1)	37 (1)	−2 (1)	43 (1)
C(13)	14586 (12)	59206 (9)	68428 (7)	289 (3)	241 (2)	125 (2)	31 (2)	−42 (2)	27 (1)
C(14)	15770 (9)	80501 (9)	87218 (9)	194 (2)	219 (2)	295 (3)	128 (2)	60 (2)	108 (2)
O(15)	36224 (6)	70002 (5)	87587 (6)	113 (1)	160 (1)	210 (1)	55 (1)	2 (1)	45 (1)

Table 6. *Final atomic coordinates* ($\times 10^5$) *and thermal parameters for hydrogen and deuterium after high-order refinement*

	x	y	z	B (Å^2)
H(O1*a*)	58250	19025	81196	11·9
H(O1*b*)	52444	15303	77776	2·1
D(C2*a*-1)	24249	33715	82334	3·0
D(C2*a*-2)	36150	35550	95995	3·0
D(C2*a*-3)	21468	18511	88591	4·2
D(C2*b*-1)	24171	30547	81540	5·1
D(C2*b*-2)	36072	32382	95201	2·0
D(C2*b*-3)	21390	15343	87797	3·7
D(C3*a*-1)	69527	45829	64970	3·8
D(C3*a*-2)	54917	51607	66357	15·6
D(C3*a*-3)	67042	51736	81285	8·8
D(C3*b*-1)	66233	44005	64418	15·6
D(C3*b*-2)	51623	49783	65805	2·1
D(C3*b*-3)	63748	49912	80733	1·9
D(C8-1)	4577	7671	32564	3·4 (9)
D(C8-2)	11983	2261	15127	3·7 (11)
D(C8-3)	25543	20705	24122	4·0 (12)
D(C9-1)	817	−16550	43425	3·7 (10)
D(C9-2)	8772	−21825	26314	3·1 (8)
D(C9-3)	19647	−19749	43075	3·7 (10)
H(O10)	48611	12563	21219	3·4 (9)
D(C13-1)	1523	56876	64857	4·7 (17)
D(C13-2)	15024	48469	67255	18·5 (435)
D(C13-3)	24697	67579	61026	4·1 (13)
D(C14-1)	1591	77133	86813	4·7 (17)
D(C14-2)	19563	86244	98469	5·5 (24)
D(C14-3)	23521	88872	78882	3·4 (9)
H(O15)	39103	72445	98308	4·9 (17)

are $R=0{\cdot}052$ and $R_w=0{\cdot}051$. The atomic parameters are given in Tables 5 and 6.

Discussion of the structure

A projection of the structure along [001] is given in Fig. 4. Molecules *A* and *A'* around an inversion centre are linked by hydrogen bonds of the type O(1)–H···O(10'). Clusters *A*–*A'* are linked to chains in the *c* direction through the hydrogen bond system O(10)–H···O(15')–H···O(1, $z-1$). Fig. 4 also shows that successive chains in the [001] direction are connected by molecules *B*, giving layers parallel to ($\bar{1}10$) (Fig. 5). Neighbouring layers are linked by van

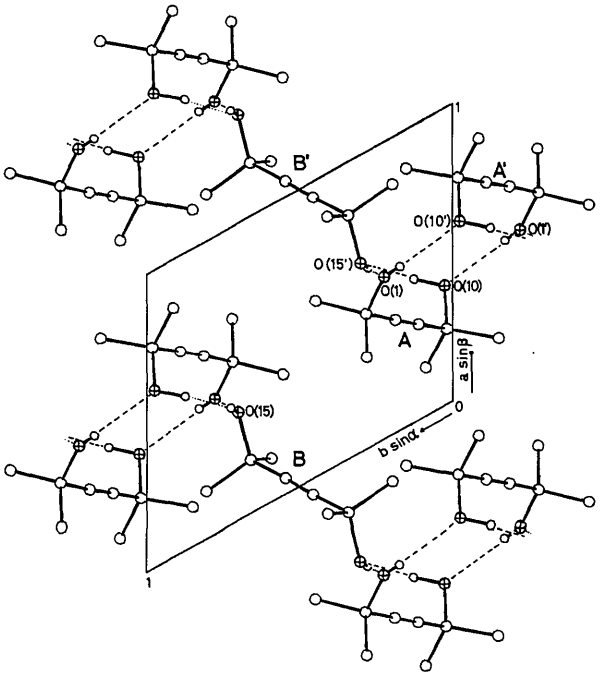

Fig. 4. Projection along [001] on to the plane perpendicular to [001]. ○ = C, ⊕ = O, ○ = H. Molecules at general position are given by *A* and *A'* (related to *A* by inversion). Molecules at special positions are indicated by *B*. D atoms of CD_3 groups are not given. For the split atoms the mean position has been taken. Hydrogen bonds are indicated by ---, but by --- and ··· if one O atom forms hydrogen bonds with two successive molecules in the *c* direction.

der Waals interactions only, which explains the easy cleavage of the crystals along ($\bar{1}10$).

The group C(4) [$OH(CD_3)_2$] with $C\cdots C \geq 3{\cdot}89$ Å lies at larger distances from the surrounding molecules than the remaining groups C[$OH(CD_3)_2$] with $C\cdots C \geq 3{\cdot}69$ Å. This can explain the large libration, or disorder, of the group C(4) [$OH(CD_3)_2$] about C(4)–C(5).

The geometry of the hydrogen bonds is given in Table 7. Two of the bonds are nearly linear. For the largest hydrogen bond only one O-atom lone pair is involved in the bonding; the other two bonds make use of both O lone pairs.

Analysis of the thermal parameters (Cruickshank, 1956) showed that the molecules cannot be considered as rigid bodies. Therefore the bond distances and angles given in Tables 7 and 8 are not corrected for libration. In agreement with the decreasing influence of the valence electrons for the HO refinement we can clearly detect trends in the bond lengths going from FA to HO. For FA C≡C is 0·004 Å shorter and C(sp)–C(sp^3) 0·002 Å longer than for HO, while C–O is 0·002 Å longer due to the lone-pair electrons of oxygen. The HO value of 1·208 Å for C≡C is approximately equal to the value of 1·206 Å found for ethyne (Lide, 1962). The C(sp)–C(sp^3) bonds, 1·474 Å, are shorter than the C–CH_3 bonds, 1·527 Å. They are larger, however, than the value of 1·459 Å found by Lide (1962). As observed in other glycols (Jeffrey & Shen, 1972; Helmholdt & Reynaers, 1976) in the groups –C(CH_3)$_2$OH the angles C–C–O are generally smaller than the angles C–C–C. The C–O lengths can be compared with the values observed by Ruysink & Vos (1974*a*) for the C–O bonds in *trans* (1·436 and 1·452 Å) and in *cis* (1·432 and 1·440 Å) 2,5-dimethyl-3-hexene-2,5-diol, with the value of 1·444 Å observed for 2,5-dimethylhexane-2,5-diol (Helmholdt & Reynaers, 1976) and with the value of 1·459 Å (Jeffrey & Shen, 1972). No explanation has yet been found for the variation in these bond lengths.

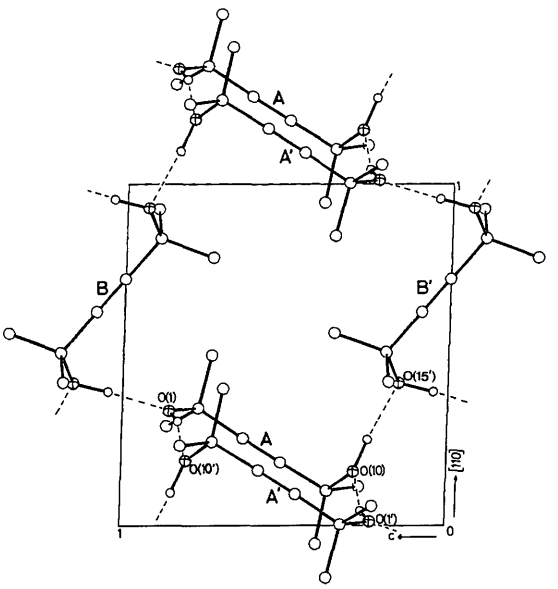

Fig. 5. Projection of one layer from Fig. 4 on to the plane ($\bar{1}10$).

Deformation densities

Sections of the [$F_o - F_c(HO_{par})$] difference map were calculated with the LO reflexions, $(\sin\theta)/\lambda \leq 0{\cdot}65$ Å^{-1}, having $|F_o| > 3\sigma(|F_o|)$. This difference density, the so-called deformation density, represents the change in density due to the formation of chemical bonds. In Figs. 6 and 7 sections through the single and triple C–C bonds are given. Fig. 8 gives information on the density in the sections perpendicular to the C≡C or C–C bonds and going through the centres of the bonds. Approximate circular symmetry is expected for the deformation density D in these sections. Fig. 8 shows the average value of $D(r)$ as a function of the distance r from the bond. The deviation from circular symmetry is given by

$$C = r(D = \tfrac{1}{2}D_{max}, \mathbf{r}_1)/r(D = \tfrac{1}{2}D_{max}, \mathbf{r}_2)$$

in which $\mathbf{r}_1$ and $\mathbf{r}_2$ are the directions in the section with the largest and smallest change in density, respectively. Fig. 9 shows sections for the lone-pair regions.

Table 7. *Geometry of the hydrogen bonds*

Distances in Å and angles in degrees. The numbering is as follows

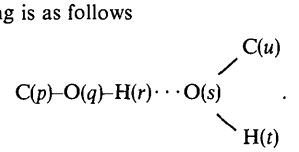

L angle between line q–s and plane s,t,u. If both lone pairs of O(s) take part in the bond $L = 0$ and if one lone pair is involved $L = 55°$.

q	s	q–s	r–s	q–r–s	p–q–r	p–q–s	t–s–u	q–s–t	q–s–u	L
O(10)	O(15′)	2·745	1·78	174	114	116·9	113	103	108·6	60
O(1)*	O(10′)	2·690	2·1†	161	115	129·4	114	122	124·1	5
O(15′)	O(1)*	2·696	1·73	177	113	114·1	115	121	123·6	9

* Based on the average position of O(1a), O(1b) and H(O1a), H(O1b).

† Inaccurate as positions of the fractional hydrogen atoms H(O1a) and H(O1b) were not constrained during the refinement.

Table 8. *Bond lengths and angles*

Standard deviations, calculated from those in Tables 3–6, × 1·5 are 0·001–0·002 Å and less than 0·12°.

	FA	HO*		FA	HO
C(4)—C(2)	(1·522)	(1·524)	O(1)–C(4)–C(2)	(106·4)	(106·7)
C(4)—C(3)	(1·525)	(1·520)	O(1)–C(4)–C(3)	(108·0)	(108·1)
C(7)—C(8)	1·529	1·529	O(1)–C(4)–C(5)	(109·8)	(109·8)
C(7)—C(9)	1·524	1·525	C(2)–C(4)–C(3)	(110·6)	(110·4)
C(12)–C(13)	1·524	1·524	C(2)–C(4)–C(5)	(110·9)	(110·8)
C(12)–C(14)	1·529	1·530	C(3)–C(4)–C(5)	(109·8)	(109·7)
⟨C–CD_3⟩	1·527	1·527	C(4)—C(5)—C(6)	178·3	178·2
			C(5)—C(6)—C(7)	178·8	178·8
			C(11′)–C(11)–C(12)	176·7	176·7
C(4)—C(5)	1·472	1·470	C(6)–C(7)–O(10)	109·4	109·4
C(6)—C(7)	1·477	1·476	C(8)–C(7)–O(10)	109·4	109·5
C(11)–C(12)	1·478	1·476	C(9)–C(7)–O(10)	106·4	106·5
⟨C(sp)–C(sp^2)⟩	1·476	1·474	C(6)–C(7)–C(8)	109·9	109·8
			C(6)–C(7)–C(9)	110·5	110·6
C(5)—C(6)	1·204	1·207	C(8)–C(7)–C(9)	111·1	110·9
C(11)–C(11′)	1·204	1·208			
⟨C≡C⟩	1·204	1·208	C(11)–C(12)–O(15)	109·6	109·8
			C(13)–C(12)–O(15)	105·7	105·5
C(4)—O(1)	(1·441)	(1·441)	C(14)–C(12)–O(15)	110·2	110·2
C(7)—O(10)	1·432	1·431	C(11)–C(12)–C(13)	110·9	110·9
C(12)–O(15)	1·434	1·431	C(11)–C(12)–C(14)	109·3	109·2
			C(13)–C(12)–C(14)	111·0	111·1
⟨C–O⟩	1·433	1·431			

* FA = full angle, HO = high order.

The standard deviation in the difference density was estimated by considering the density at positions far removed from chemical bonds. The maximum value observed, 0·075 e $Å^{-3}$, was considered as $3\sigma(D)$ so that $\sigma(D)$ was estimated at 0·025 e $Å^{-3}$. This estimate may be too high as analysis of the map showed that the r.m.s. variation of the maxima on the single C–C bonds is as small as 0·015 e $Å^{-3}$. Systematic errors in the density can occur due to (*a*) a small correlation between parameters and bonding effects in the HO refinement, (*b*) the restricted number of reflexions used in the calculation of the map, and (*c*) the neglect of TDS corrections. A rough estimate of the errors due to (*a*) was made by comparing deformation densities in the $D[X-N]$ and $D[X-X(\mathrm{HO})]$ maps of sucrose (Hanson *et al.*, 1973). As sucrose is acentric and III-D is centric the observed differences were divided by two. The comparison suggests that as a result of (*a*) the maxima on C–C (and as we assume also on C≡C; see next section, however) and C–O will be roughly 10% too low, whereas the lone pairs are 25% too low.

An example of the low resolution of the map due to (*b*) will be given in the next section. An estimate of the erros due to (*c*) has been made by Helmholdt & Vos (1977) for a model consisting of spherically symmetric atoms by doing TDS calculations in the long-wave approximation. For the centres of the bonds and at the atomic positions errors ranging from 0·00–0·03 and 0·05–0·08 e $Å^{-3}$, respectively, are expected. It should be noted, however, that for the model assumed the

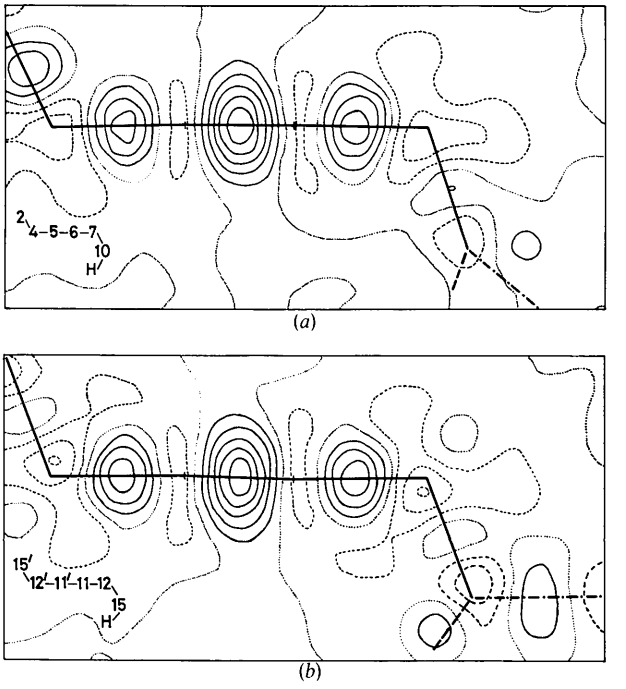

Fig. 6. Low-angle deformation density in the planes through C(4), C(7) and O(10) (*a*) and C(12′), C(12) and O(15) (*b*). --- projection of OH bond on to the plane. ----- projection of O···O direction of the H-bridge on to the plane. —— bonds between atoms less than 0·05 Å from the plane [C(2)–C(4) is by accident in the plane of (*a*)]. In all figures contours at intervals of 0·1 e $Å^{-3}$: ··· zero, —— positive, --- negative density.

deformation density is zero, whereas in reality at the centres of the bonds maxima are observed. Neglect of TDS corrections makes these maxima too high, as TDS errors cause the apparent thermal motion and thus the smearing of the density to be too small (de With, 1976). This latter error does not influence, however, the comparison of the experimental deformation density with theoretical dynamic densities, if for the theoretical model the thermal motion is adjusted as much as possible to the experimental thermal parameters.

In the discussion of the next section the experimental deformation density will be compared with a theoretical density (Fig. 10). Use was made of the model compound

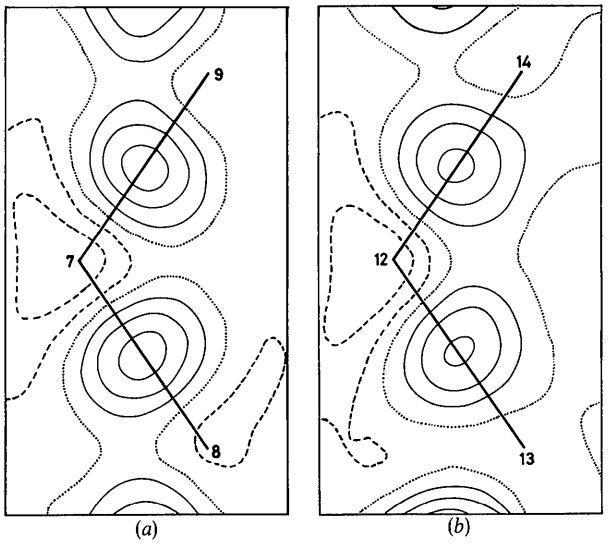

Fig. 7. Low-angle deformation density in the planes P = C(8)–C(7)–C(9) (*a*) and Q = C(13)–C(12)–C(14) (*b*).

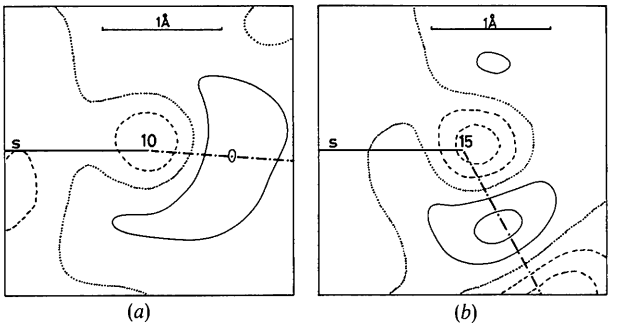

Fig. 9. Low-angle deformation densities around the oxygen atoms. (*a*) The plane Bis (the plane of the figure) bisects the angle C(7)–O(10)–H(O10). ----- projection of O(10)···O(15′) on Bis; *s* is the line of intersection of Bis and the plane through C(7), O(10) and H(O10). (*b*) Analogous situation for C(12)–O(15)–H(O10).

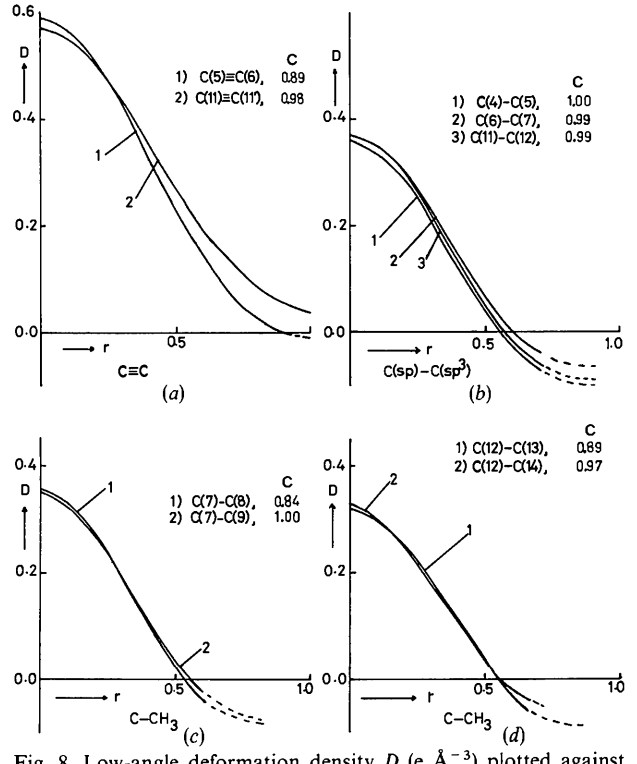

Fig. 8. Low-angle deformation density D (e Å^{-3}) plotted against r (Å) in the plane perpendicular to a bond and going through the centre of the bond. For definition of C see text.

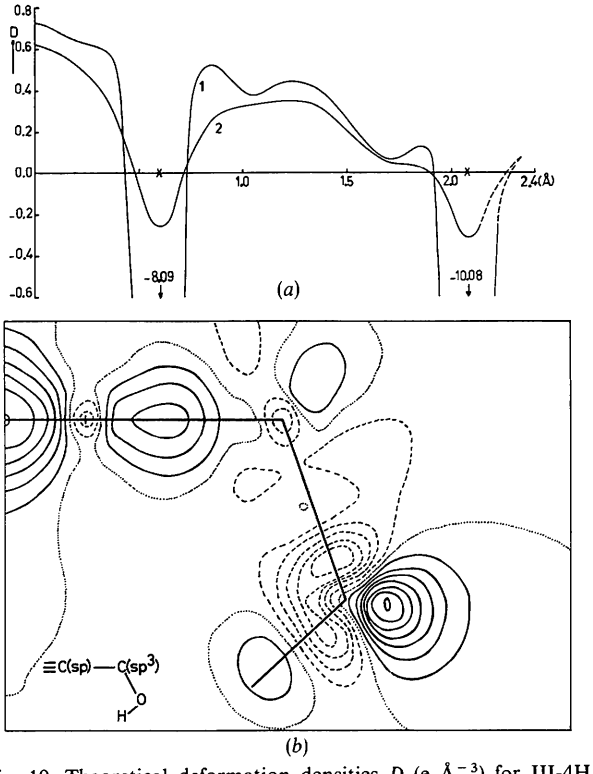

Fig. 10. Theoretical deformation densities D (e Å^{-3}) for III-4H. (*a*) Along ≡C–C. Curve 1: static model; curve 2: dynamic model, × atomic positions. Centre of C≡C lies at zero. (*b*) Dynamic density in the symmetry plane.

2,4-diol-2-butyn (III-4H) for which the symmetry 2/*m* was assumed. The (rigid-body) translations and librations of the model were adjusted as much as possible to the thermal motion of III-D. The static density was obtained by *ab initio* calculations in which a small (6,3/3) GTO basis set was used. From this density the dynamic density was calculated according to the method described by Ruysink & Vos (1974*b*).

In the theoretical density errors will occur due to the use of the small basis set. From a comparison of the deformation densities obtained for ethyne from a restricted (6,3/3) and an extended (10,6,2/5,2) GTO set, Ruysink (1973) has concluded that for the small set the density at the centre of C≡C is approximately 10% too low.

From the discussion given above we expect that, apart from TDS effects, both for the experimental and theoretical deformation densities the values of the maxima on the (single and triple) C–C bonds are roughly 10% too low (owing to correlation and the small basis set respectively). It is therefore possible to make a direct comparison of the experimental and theoretical C–C maxima.

Discussion of the deformation density

Figs. 6–8 show that the deformation densities are very similar for the two molecules. From a comparison of the experimental density of Fig. 6 and the theoretical density of Fig. 10(*b*), we see that there are analogous features, but also differences between the experimental and theoretical maps.

Single and triple C–C *bonds*

Figs. 6 and 10(*b*) show that both the experimental and theoretical maps have positive densities on the C–C bonds and negative values around the positions of the C atoms and at either side of the C–C≡C–C bonding region. Positive values are also observed on the C–CH_3 bonds of Fig. 7, whereas near the C atoms of these bonds and also near the C atoms of the C–O bonds (Fig. 6) negative regions occur which are pointing away from the bonds.

The values at the centres of the C–C bonds (Fig. 6), with theoretical values in parentheses, are 0·58 (0·62) for C≡C and 0·37 (0·35) e $Å^{-3}$ for C(*sp*)–C(sp^3). The ratio between the experimental and theoretical values is 0·94 for C≡C and 1·06 for C–C. The relatively small experimental value at C≡C will be due mainly to the (small) correlation between the HO C(*sp*) position and bonding effects. If we assume that at C≡C and C–C the theoretical maxima are 10% too low as a result of the small basis set and that the difference between the ratios is completely due to correlation, we see that correlation reduces the maxima at C≡C and C–C in the unit C–C≡C–C by about 15 and 4% respectively. This may be compared with the 10% estimated in the previous section from the sucrose deformation density maps.

At the C(*sp*) atoms the *D* values are between −0·09 and −0·12 (−0·26) e $Å^{-3}$ and at the atoms of type C(4) approximately −0·29 (−0·31) e $Å^{-3}$. Moreover Figs. 6 and 10(*b*) show that the minima at the C atoms, especially that at C(*sp*), are much sharper in the theoretical map than in the experimental map. We ascribe this difference in height and in steepness mainly to the restricted resolution of the experimental map, which especially influences the deformation densities close to the atomic positions (Ruysink, 1973).

Both in the experimental maps of Fig. 6 and in the theoretical map of Fig. 10(*b*), the positive region around C≡C is extended strongly in the direction perpendicular to C≡C. Fig. 8 shows that the radial density distributions of bonds of the same type do not show large differences. As expected, the heights of the maxima are influenced by the thermal motion. Fig. 7 shows that for group *Q*, which has a slightly larger thermal motion than *P*, the density is smeared out more and the maxima on the bonds are slightly lower than for *P*. The asymmetry parameters in Fig. 8 may be compared with the theoretical values, 0·93 for C≡C and 0·90 for C(*sp*)–C(sp^3). It is seen from Fig. 8 that the positive regions around C≡C are not only higher but also more extended in the direction perpendicular to the bond than the positive regions around the single C–C bonds.

We have tried to estimate the total number of electrons in the positive regions around the C–C bonds. To this end cylindrical symmetry was assumed for the density. In each section perpendicular to a bond the average of $D(r)$ is approximated as well as possible by the function $D(r)=C\exp(-Ar^2)-B$. The integration in each section is done from $r=0$ (on the bond) to $r=r_{max}$, where $r_{max}=r$ $(D=0)$ if the positive region is surrounded by a negative region and $r_{max}=r_{est}$ if two positive regions merge into each other. Especially in the latter case there is an uncertainty in the estimate of r_{max}. All sections with positive *D* values in the bonds were considered and the values of the successive sections added by numerical integration. Average experimental values obtained for the number of electrons. on the bonds are 0·28 for C≡C, 0·07 for C(*sp*)–C(sp^3) and C–CH_3. The theoretical values are 0·27 for C≡C and 0·07 for C(*sp*)–C(sp^3). The good agreement between theoretical and experimental values shows that for the integrated bond densities the experimental errors due to correlation and series termination are approximately equal to the theoretical errors due to the restricted basis set.

C–O *bonds and lone pairs*

Figs. 6 and 10 show that experiment and theory give very different deformation densities around the O atoms. In the theoretical map the O atom lies on a steep slope and it is therefore to be expected that even in a HO refinement there is an appreciable correlation between the position of the O atom and bonding effects. In the experimental map this correlation decreases the slope at the O atom. Moreover, the slope will be reduced by the finite (low-order) resolution of

the map. In the theoretical map errors will occur around O as a result of the use of the small basis set, especially the neglect of polarization functions. The experimental sections of Fig. 9 show a positive deformation density in the O-atom lone-pair region. We see that the lone-pair electrons have a tendency to concentrate around the hydrogen bonds. The same phenomenon is observed in cyanuric acid for one of the O···H–N bridges (Verschoor, 1967, Figs. 6–10), but was not pointed out by the author as the effect is hardly significant.

C–D *and* O–H *bonds*

The deformation densities at the C–D and O–H bonds are less accurate than for the C–C and C–O bonds, as the positions of the D(H) atoms were constrained during the refinement. The maximum values near the C–D bonds range from 0·14–0·30 e $Å^{-3}$, except for C(13)–D(C13-2) for which this value is 0·57 e $Å^{-3}$. This may be caused by the high B value (inaccurate position?) for D(C13-2). The maxima on the O–H bonds are 0·17 and 0·35 e $Å^{-3}$.

The authors thank Mr F. van Bolhuis for his technical assistance and Drs G. J. H. van Nes and Dr A. F. J. Ruysink for performing the quantum-mechanical calculations. One of us (RBH) acknowledges support from the Dutch Organization for the Advancement of Pure Research (ZWO). The computations were done at the Computing Centre of the University of Groningen.

References

AZAROFF, L. V. (1955). *Acta Cryst.* **8**, 701–704.
BOER, J. L. DE (1974). Private communication.
BOLHUIS, F. VAN (1971). *J. Appl. Cryst.* **4**, 263–264.
BUSING, W. R. & LEVY, H. A. (1967). *Acta Cryst.* **22**, 457–464.
COPPENS, P. (1968). *Acta Cryst.* A**24**, 253–257.
CRUICKSHANK, D. W. J. (1956). *Acta Cryst.* **9**, 754–756.
DOYLE, P. A. & TURNER, P. S. (1968). *Acta Cryst.* A**24**, 390–397.
HANSON, J. C., SIEKER, L. C. & JENSEN, L. H. (1973). *Acta Cryst.* B**29**, 797–808.
HELMHOLDT, R. B. & REYNAERS, H. (1976). *Acta Cryst.* B**32**, 2243–2245.
HELMHOLDT, R. B., RUYSINK, A. F. J., REYNAERS, H. & KEMPER, G. (1972). *Acta Cryst.* B**28**, 318–319.
HELMHOLDT, R. B. & VOS, A. (1976). *Acta Cryst.* A**32**, 669.
HELMHOLDT, R. B. & VOS, A. (1977). *Acta Cryst.* To be published.
HOPE, H. (1971). *Acta Cryst.* A**27**, 392–393.
JEFFREY, G. A. & SHEN, M. S. (1972). *J. Chem. Phys.* **57**, 56–61.
KARLE, J. & KARLE, I. L. (1966). *Acta Cryst.* **21**, 849–868.
LIDE, D. R. (1962). *Tetrahedron*, **17**, 125–134.
MILDNER, P. & WEEDON, B. C. L. (1953). *J. Chem. Soc.* pp. 3294–3298.
O'CONNELL, A. M. (1969). *Acta Cryst.* B**25**, 1273–1280.
RUYSINK, A. F. J. (1973). Thesis, University of Groningen.
RUYSINK, A. F. J. & VOS, A. (1974*a*). *Acta Cryst.* B**30**, 1997–2002.
RUYSINK, A. F. J. & VOS, A. (1974*b*). *Acta Cryst.* A**30**, 503–506.
STEWART, J. M., KRUGER, G. J., AMMON, H. L., DICKINSON, C. & HALL, S. R. (1972). The X-RAY System – version of June 1972. Tech. Rep. TR-192. Computer Science Center, Univ. of Maryland, College Park, Maryland.
STEWART, R. F., DAVIDSON, E. R. & SIMPSON, W. T. (1965). *J. Chem. Phys.* **42**, 3175–3187.
VERSCHOOR, G. C. (1967). Thesis, University of Groningen.
WHITTAKER, E. & ROBINSON, G. (1949). *The Calculus of Observations*. London: Blackie.
WITH, G. DE (1976). *Acta Cryst.* B**32**, 3178–3184.
ZACHARIASEN, W. H. (1967). *Acta Cryst.* **23**, 558–564.
ZACHARIASEN, W. H. (1968). *Acta Cryst.* A**24**, 212–216.